JOURNAL OF Materials CHEMISTRY

Antiferromagnetic properties of the intermetallics $Ce_3Ni_2X_7$ ($X = Ge$ or Sn)

B. Chevalier* and J. Etourneau

Institut de Chimie de la Matière Condensée de Bordeaux (ICMCB), CNRS [UPR 9048], Université Bordeaux I, Avenue du Docteur A.Schweitzer, 33608 Pessac Cedex, France. E-mail: chevalie@icmcb.u-bordeaux.fr

Received 10th March 1999, Accepted 13th May 1999

Electrical resistivity and magnetization measurements have been performed on the isotypic compounds $Ce_3Ni_2Ge_7$ and $Ce_3Ni_2Sn_7$. The ternary germanide orders antiferromagnetically below $T_N = 7.0(2)$ K, a Néel temperature higher than that observed for $Ce_3Ni_2Sn_7$ [$T_N = 3.8(2)$ K]. This investigation allows proposal of a direct relationship between the Ce valence and the smallest interatomic distances d_{Ce-Ni} and d_{Ce-Sn} for the ternary stannides existing in the Ce–Ni–Sn system.

1 Introduction

The ternary compounds $Ce_3Ni_2Ge_7$ and $Ce_3Ni_2Sn_7$ have been prepared[1,2] and their investigation by X-ray powder diffraction reveals that they adopt the orthorhombic $La_3Co_2Sn_7$-type structure (*Cmmm* space group).[3] This structure can be considered as an intergrowth combining three different polyhedra (Fig. 1): (i) a cubooctahedron [Ge_{12} or Sn_{12}] surrounding a Ce atom; (ii) an antiprism [Ce_4Ge_4 or Ce_4Sn_4] occupied by a Ni atom; (iii) a trigonal prism [Ce_6] within which an Sn atom is located. Similar coordination polyhedra exist in other structures of cerium-based intermetallics such as [Sn_{12}]-cubooctahedra in cubic $CeSn_3$[4] ($AuCu_3$-type) and both a [Ce_6]-trigonal prism and a [Ce_4Ge_4]- or [Ce_4Sn_4]-antiprism in orthorhombic $CeNi_{1-x}Ge_2$ and $CeNi_{1-x}Sn_2$[2,5] ($CeNiSi_2$-type). These latter compounds show interesting physical properties since cerium in $CeSn_3$ exhibits an intermediate valence character[4] and $CeNiGe_2$ and $CeNiSn_2$ are considered as 'heavy-fermion' antiferromagnets.[6,7] Therefore, it was of interest to determine the physical properties of $Ce_3Ni_2Ge_7$ and $Ce_3Ni_2Sn_7$ which show a structural relationship with these intermetallics.

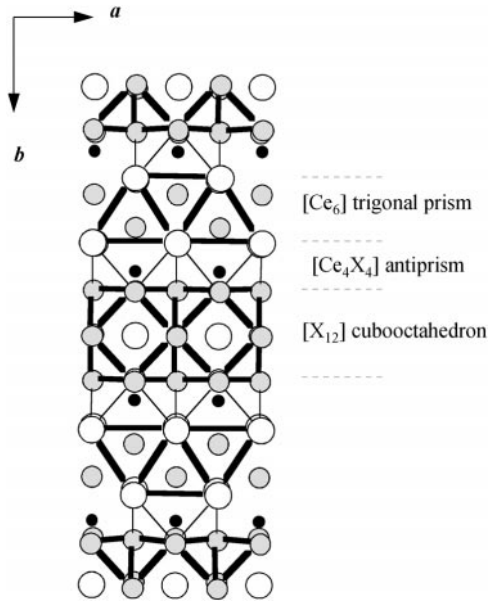

Fig. 1 Projection along the *c*-axis of the crystal structure of $Ce_3Ni_2X_7$ with X = Ge or Sn (Ce, X and Ni atoms are respectively represented by large white, medium grey and small black circles).

Here we report their synthesis, crystal structure and electrical and magnetic properties. We comment more particularly on the structural investigation of $Ce_3Ni_2Sn_7$ from an X-ray powder diffraction study and show that the physical properties of the stannides existing in the Ce–Ni–Sn system are governed by the d_{Ce-Ni} and d_{Ce-Sn} interatomic distances.

2 Experimental

The samples were synthesized by melting stoichiometric quantities of the constituents (purity >99.9%) in an induction levitation furnace under a purified argon atmosphere. Then, the samples were sealed in a quartz tube under vacuum and annealed for five weeks at 800 °C.

Microprobe analysis was used to check both the homogeneity and the composition of the samples obtained after melting or annealing. The analysis was based on the measurements of the Ce-Lα_1, Ni-Kα_1, Ge-Kα_1 and Sn-Lα_1 X-ray emission lines, which were compared with those obtained for CeNiGe and CeNiSn used as references. This analysis indicates that the two as-cast samples are a mixture containing mainly Ge and $CeNiGe_2$ for the germanide and $CeNi_{0.5}Sn_2$ for the stannide. This result indicates clearly that these intermetallics do not melt congruently. By contrast, the annealed samples exhibit good chemical homogeneity and are single phases. The experimental atomic percentages are respectively: Ce 23.6(4)%; Ni 19.7(3)% and Ge 56.7(4)% for $Ce_3Ni_2Ge_7$ and Ce 24.5(3)%; Ni 17.0(3)% and Sn 58.5(4)% for $Ce_3Ni_2Sn_7$. These percentages are close to the theoretical values (Ce 25.0%; Ni 16.7%; Ge or Sn 58.3%) for the ternary stannide but an excess of nickel is present in the germanide.

All the samples were also examined by X-ray powder diffraction (Guinier camera, Cu-Kα radiation). The unit cell parameters were determined by a least-squares refinement method using silicon (5N) as an internal standard. The crystal structure of $Ce_3Ni_2Sn_7$ was refined by the Rietveld profile method.[8] The data were collected on a Philips PW 1050 diffractometer using Bragg–Brentano geometry with Cu-Kα radiation and a take-off angle of 6°. The pattern was scanned in steps of 0.02° (2θ) from 15 to 120° with a constant counting time of 30 s.

Magnetization measurements were performed using a Superconducting QUantum Interference Device (SQUID) magnetometer in the temperature range 1.8–300 K and applied fields up to 5 T. Electrical resistivity was determined above 4.2 K on polycrystalline samples using standard dc four probe measurements.

Table 1 Atomic parameters for $Ce_3Ni_2Sn_7$ (space group *Cmmm*, unit cell parameters: $a=4.5650(2)$, $b=27.3041(9)$ and $c=4.5690(2)$ Å)

Atom	Site	x	y	z	B/Å^2
Ce(1)	2d	0	0	1/2	0.21(1)
Ce(2)	4i	0	0.3147(2)	0	0.21(1)
Ni(1)	4j	0	0.1290(3)	1/2	0.38(2)
Sn(1)	2b	1/2	0	0	0.32(2)
Sn(2)	4j	0	0.4095(1)	1/2	0.32(2)
Sn(3)	4i	0	0.0890(2)	0	0.32(2)
Sn(4)	4j	0	0.2168(2)	1/2	0.32(2)

3 Results and discussion

3.1 Structural properties

X-Ray powder diffraction performed on a $Ce_3Ni_2Ge_7$ annealed sample revealed only peaks corresponding to the expected orthorhombic $La_3Co_2Sn_7$ structure. The unit cell parameters $a=4.238(2)$, $b=25.76(1)$ and $c=4.285(2)$ Å are in agreement with those determined previously.[1]

The stannide $Ce_3Ni_2Sn_7$ is considered as isostructural with $La_3Co_2Sn_7$ from its X-ray powder pattern. The crystallographic parameters (unit cell and atomic coordinates), determined from the Rietveld profile refinement of the X-ray data are listed in Table 1. After refinement, the values of the reliability factors R_F, R_p and R_{wp} were 0.067, 0.122 and 0.169, respectively.

In the structure of $Ce_3Ni_2Sn_7$, Ce atoms occupy two non-equivalent positions (Fig. 1): the first [Ce(1)] has a coordination polyhedron ([Sn_{12}]-cubooctahedron) resembling that observed in $CeSn_3$[4] whereas the second [Ce(2)] has the same environment as in $CeNi_{1-x}Sn_2$ stannides.[5,9] Interatomic distances relating to these Ce atoms are given in Table 2. The smallest d_{Ce-Sn} spacing (3.229 Å) is clearly shorter than that found in $CeSn_3$ (3.339 Å).[4]

3.2 Electrical properties

Fig. 2 shows the thermal dependence above 4.2 K of the reduced electrical resistivity of $Ce_3Ni_2Ge_7$ and $Ce_3Ni_2Sn_7$. (Owing to the presence of microcracks in the polycrystalline samples, absolute values of $\rho(T)$ could not be determined accurately; for this reason, reduced resistivity is reported.) Above 20 K, the reduced resistivity of $Ce_3Ni_2Ge_7$ does not vary linearly with temperature (as for a normal metal) and the curve $\rho(T)/\rho(270\ K)=f(T)$ presents a downward curvature associated with a crystal-field effect which becomes temperature dependent in the paramagnetic range. At low temperatures its reduced resistivity increases slightly between 20 and 8 K then decreases strongly. This behaviour is typical of a magnetically ordered Kondo system showing the presence of crystal field splitting of the 4f(Ce) electron. No anomaly can be detected from the curve $\rho(T)/\rho(270\ K)=f(T)$ for $Ce_3Ni_2Sn_7$; only a less pronounced downward curvature is observed with no tendency to saturation at low temperature. This strikingly different behaviour indicates the absence of Kondo scattering as found in $Ce_3Ni_2Ge_7$.

Table 2 Selected interatomic distances for $Ce_3Ni_2Sn_7$

Ce(1)–Ce(1) 4.5650(2) (×2)	Ce(2)–Ce(2) 4.5650(2) (×2)
–Ce(1) 4.5690(2) (×2)	–Ce(2) 4.5690(2) (×2)
–Sn(1) 3.2294(5) (×4)	–Ce(2) 4.2063(2) (×2)
–Sn(3) 3.3353(5) (×4)	–Sn(4) 3.3419(5) (×4)
–Sn(2) 3.3639(5) (×4)	–Sn(4) 3.5163(5) (×2)
–Ni 3.5222(5) (×2)	–Sn(2) 3.4524(5) (×2)
	–Sn(3) 3.4819(5) (×2)
	–Ni 3.5766(5) (×4)

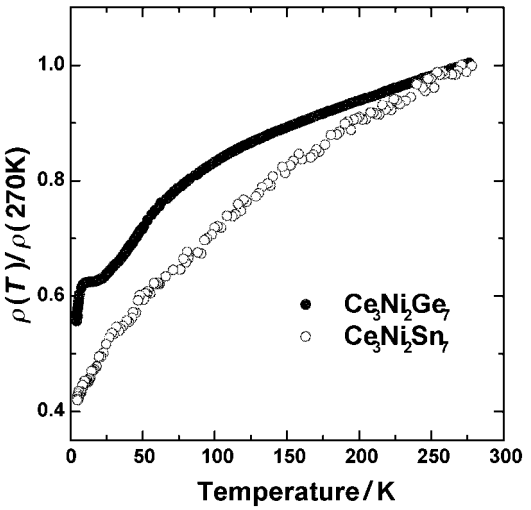

Fig. 2 Temperature dependence of the reduced electrical resistivity of $Ce_3Ni_2Ge_7$ and $Ce_3Ni_2Sn_7$.

3.3 Magnetic properties

Fig. 3 shows the thermal dependence of the reciprocal magnetic susceptibility χ_m^{-1} measured with an applied field of 1 T. Above 70 and 40 K respectively for $Ce_3Ni_2Ge_7$ and $Ce_3Ni_2Sn_7$, the data can be fitted with a Curie–Weiss law $\chi_m^{-1}=(T-\theta_p)/C_m$ giving $\theta_p=-20$ K and $\mu_{eff}=(8C_m/3)^{1/2}=2.32\ \mu_B$/Ce for $Ce_3Ni_2Ge_7$ and $\theta_p=-13$ K and $\mu_{eff}=2.33\ \mu_B$/Ce for $Ce_3Ni_2Sn_7$. The curvature observed at low temperatures in the $\chi_m^{-1}=f(T)$ curves indicates the presence of a crystal-field effect. The negative value of the paramagnetic Curie temperature θ_p suggests the predominance of antiferromagnetic interactions for these compounds. The effective moment values are slightly lower than that calculated for a free Ce^{3+} ion (2.54 μ_B).

From the study of the electrical and magnetic properties of $Ce_3Ni_2Sn_7$, Skolozdra[2,10] claimed that this ternary stannide is an intermediate valence system. By contrast, our investigation shows that the cerium is trivalent in $Ce_3Ni_2Sn_7$. We note that Skolozdra[10] performed magnetic measurements only above 77 K.

The thermal dependence of the magnetic susceptibility χ_m of $Ce_3Ni_2Ge_7$ and $Ce_3Ni_2Sn_7$ (Fig. 4) measured at a low field of 0.05 T shows a peak typical of an antiferromagnetic ordering, with $T_N=7.0(2)$ and 3.8(2) K, respectively. With increasing magnetic field at 2 K, the magnetization of these

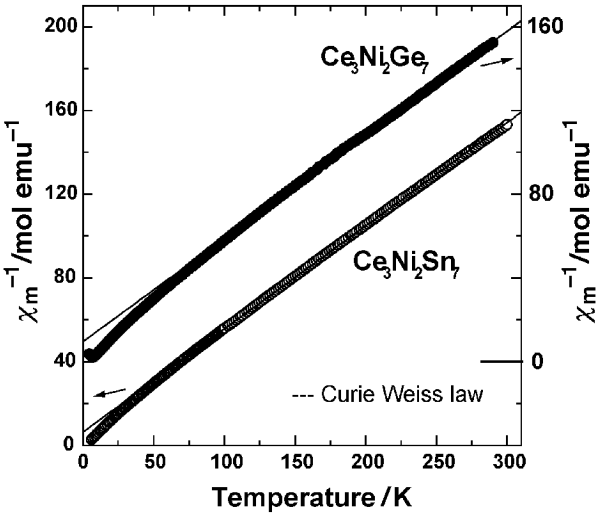

Fig. 3 Temperature dependence of the reciprocal magnetic susceptibility of $Ce_3Ni_2Ge_7$ and $Ce_3Ni_2Sn_7$ (for clarity the curve relative to $Ce_3Ni_2Ge_7$ is shifted vertically).

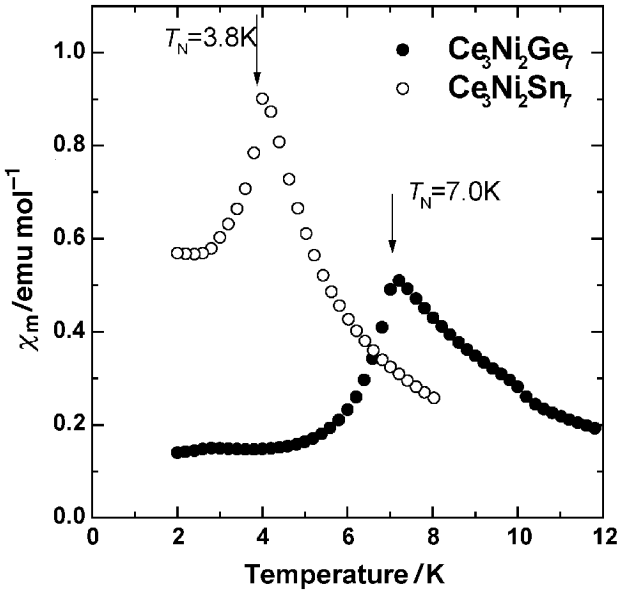

Fig. 4 Temperature dependence of the magnetic susceptibility of $Ce_3Ni_2Ge_7$ and $Ce_3Ni_2Sn_7$ measured in a field of 0.05 T.

compounds increases linearly at low fields, shows a steep rise in the range 0.4–0.6 T and then exhibits a tendency to saturation (Fig. 5). This behaviour is typical of a metamagnetic transition; at 2 K the critical field is estimated at *ca.* 0.6 and 0.4 T for the germanide and stannide, respectively.

It is of note that T_N of $Ce_3Ni_2Ge_7$ is higher than that observed for the stannide $Ce_3Ni_2Sn_7$. This result is surprising because as a general rule, cerium–nickel-based germanides are less magnetic than the corresponding stannides. For example, in the sequence CeNiGe→CeNiSn a transition from an intermediate valence state to Kondo semiconductor behaviour is observed;[11,12] in the same way $CeNi_2Ge_2$ is considered as a non-ordered 'heavy-fermion' system[13] whereas $CeNi_2Sn_2$ orders antiferromagnetically below $T_N=1.8$ K[14] with a reduced Ce magnetic moment of 0.90(12) μ_B.[15] However, $CeNiGe_2$ and $CeNiSn_2$ have an identical Néel temperature $T_N\cong3.9$ K.[7] It is well known that the magnetic properties of these compounds are governed by the competition between the Kondo interaction which tends to demagnetize 4f(Ce) states and the magnetic RKKY-interaction which drives the system towards a long-range magnetic ordering. The two types of interaction depend on J_{cf} which is the interaction constant between the spins of localized 4f(Ce)

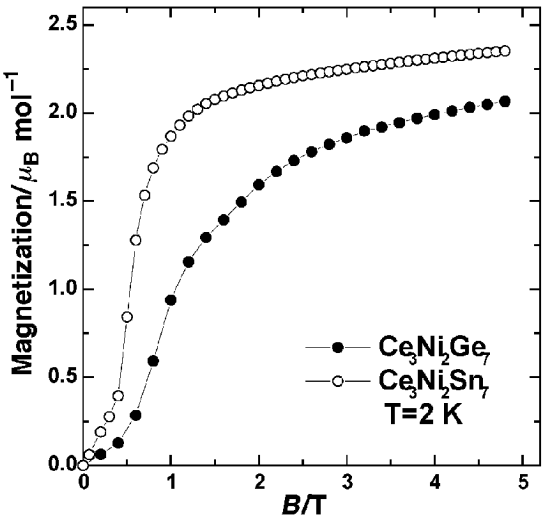

Fig. 5 Field dependence at 2 K of the magnetization of $Ce_3Ni_2Ge_7$ and $Ce_3Ni_2Sn_7$.

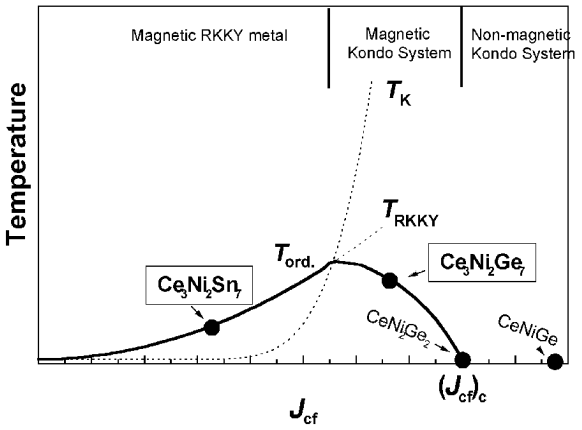

Fig. 6 Schematic Doniach's phase diagram for a concentrated Kondo system.

electrons and conduction electrons. The strength of J_{cf} depends on both a structural factor (interatomic distances) and an electronic factor [$N(0)$ density of states at the Fermi level]. According to this view, Doniach has proposed a magnetic phase diagram (Fig. 6) showing at $T=0$ K, the occurrence of a second-order phase transition at a critical value $J_{cf}=(J_{cf})_c$ separating the magnetic Kondo ground state from the fully spin-compensated ground state (Kondo metal):[16] (i) for small J_{cf}, the magnetic ordering temperature $T_{RKKY}\propto N(0)\,J_{cf}^2/k_B$ is larger than $T_K\propto[k_BN(0)]^{-1}\,e^{-1/N(0)\,J_{cf}}$ characterizing the Kondo effect; (ii) for larger J_{cf}, the Kondo effect is strong leading to $T_K\gg T_{RKKY}$. This diagram indicates that, with increasing J_{cf}, the magnetic ordering temperature T_{ord} increases initially, then goes through a maximum and finally decreases rapidly by driving the system to a non-magnetic Kondo state. From the Néel temperatures of $Ce_3Ni_2Ge_7$ and $Ce_3Ni_2Sn_7$ we can state that the interaction constant J_{cf} is greater in the germanide than in the stannide as previously observed for CeNiGe and CeNiSn on one hand and for $CeNi_2Ge_2$ and $CeNi_2Sn_2$ on the other: (i) the unit cell volume of $Ce_3Ni_2Ge_7$ ($V_m=467.80$ Å^3) is smaller than that determined for $Ce_3Ni_2Sn_7$ ($V_m=569.49$ Å^3) indicating a greater hybridization between 4f(Ce) and the conduction electron states in the germanide; (ii) in addition the germanide shows Kondo behaviour unlike the stannide. Under these conditions, the higher T_N temperature of $Ce_3Ni_2Ge_7$ can be explained by the J_{cf} value occurring in the magnetic Kondo system range of Doniach's diagram (Fig. 6).[16] In Fig. 6, we have positioned $CeNi_2Ge_2$ and CeNiGe according to their physical properties: J_{cf} for $CeNi_2Ge_2$ is very close to

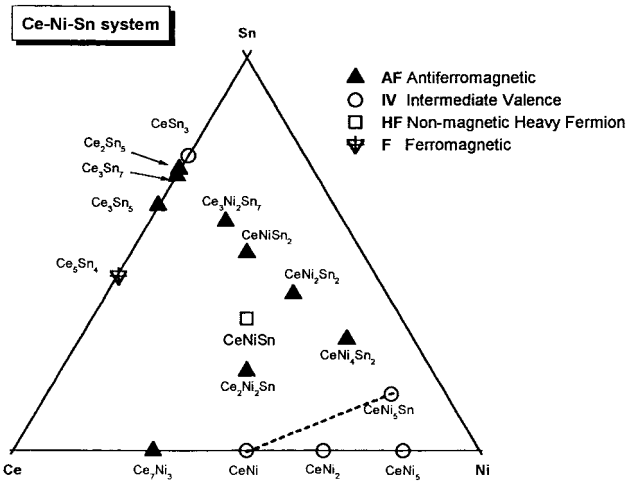

Fig. 7 Magnetic properties of some binary and ternary compounds in the Ce–Ni–Sn system (the dotted line shows the border between trivalent and intermediate valence states of cerium).

Table 3 Relationships between Ce valence and smallest interatomic distances $d_{Ce–Ni}$ and $d_{Ce–Sn}$ for binary and ternary compounds existing in the Ce–Ni–Sn system (Ce IV = Ce in intermediate valence; AF = antiferromagnetic)

		Smallest distance/Å			
	Compound	$d_{Cd–Ni}$	$d_{Cd–Sn}$	Physical behaviour	Ref.
Ce IV	$CeNi_5$	2.806		Pauli paramagnet	18, 19
	$CeNi_5Sn$	2.832	3.210	Pauli paramagnet	17, 20, 21
	CeNi	2.890		Pauli paramagnet	19, 22
Ce (trivalent state)	Ce_2Ni_2Sn	3.027	3.359	Kondo AF, $T_N = 4.7$ K	21, 23
	CeNiSn	3.064	3.183	Kondo insulator	12, 24
	$CeNi_4Sn_2$	3.087	3.500	AF, $T_N = 11.0$ K	17, 25, 26
	$CeNi_2Sn_2$	3.306	3.361	Kondo AF, $T_N = 1.8$ K	14, 15, 27
	$CeNi_{0.84}Sn_2$	3.456	3.397	AF, $T_N = 4.0$ K	9, 28
	$Ce_3Ni_2Sn_7$	3.522	3.229	AF, $T_N = 3.8$ K	This work
Ce IV	$CeSn_3$		3.339	Pauli paramagnet	4

the critical value $(J_{cf})_c$ since this ternary germanide is a non-magnetic 'heavy-fermion',[13] whereas CeNiGe, which is a Pauli paramagnet, has a higher J_{cf} value.[11]

3.4 Interplay between structural and physical properties in the Ce–Ni–Sn system

Fig. 7 shows a proposed Ce–Ni–Sn phase diagram indicating the physical behaviour of all ternary stannides known so far, as a function of their chemical composition. Several features can be seen: (i) the binary compounds on the Ni-rich side (CeNi, $CeNi_2$ and $CeNi_5$) and the richest ternary stannide for nickel ($CeNi_5Sn$) exhibit an intermediate valence character (the magnetic susceptibility of this last stannide is practically independent of temperature and its spin-fluctuation temperature is high, $T_K \cong 500$ K[17]); (ii) the dotted line connecting CeNi to $CeNi_5Sn$ separates the domain where Ce exhibits an intermediate valence state from that where Ce is trivalent; (iii) except for CeNiSn which shows a non-magnetic 'heavy-fermion' behaviour, all the other ternary stannides located on the left of this dotted line are antiferromagnets.

Table 3 shows how the Ce valence in these binary and ternary compounds is connected to the value of the smallest interatomic distances $d_{Ce–Ni}$ and $d_{Ce–Sn}$ existing between Ce and neighbouring Ni and Sn atoms. It is well known that these spacings govern the strength of 4f(Ce)–3d(Ni) or –5p(Sn) interactions responsible for the electronic state of cerium. Several points can be made from Table 3: (i) the three compounds $CeNi_5$, $CeNi_5Sn$ and CeNi corresponding to the Ni richest compositions, exhibit the shortest $d_{Ce–Ni}$ distance and show an intermediate valence behaviour; we note also that $CeNi_5Sn$ has a $d_{Ce–Sn}$ distance much shorter than that in the binary intermediate valence stannide $CeSn_3$; (ii) an increase of the $d_{Ce–Ni}$ distances leads to a trivalent state for cerium with the occurrence of an antiferromagnetic ordering, except for CeNiSn which shows Kondo insulator behaviour without magnetic ordering down to 2 K,[12] CeNiSn exhibits one of the shortest $d_{Ce–Ni}$ distances and the smallest $d_{Ce–Sn}$ distance observed in this series of ternary compounds.

4 Conclusion

This study has shown that $Ce_3Ni_2Ge_7$ orders antiferromagnetically at $T_N = 7.0(2)$ K, *i.e.* at a temperature higher than that observed for the corresponding ternary stannide $Ce_3Ni_2Sn_7$ [$T_N = 3.8(2)$ K]. This observation suggests that the J_{cf} interaction is largest for the germanide. In order to check this assumption, an electronic band structure calculation based on spin polarised density functional theory[29] is now in progress for these two intermetallics. Moreover, it was observed that the physical properties (intermediate valence state, non-magnetic 'heavy-fermion' behaviour, antiferromagnetic ordering) of the ternary stannides existing in the Ce–Ni–Sn system are mainly governed by their $d_{Ce–Ni}$ distances.

References

1 P. Salamakha, M. Konyk, O. Sologub and O. Bodak, *J. Alloys Compd.*, 1996, **236**, 206.
2 R. V. Skolozdra, in *Handbook on the Physics and Chemistry of Rare Earths*, ed. K. A. Gschneidner Jr. and L. Eyring, Elsevier, North-Holland, 1997, **24**, 399.
3 W. Dörrscheidt and H. Schäfer, *J. Less-Common Met.*, 1980, **70**, 1.
4 J. Lawrence, *Phys. Rev. B*, 1979, **20**, 3770.
5 M. Francois, G. Venturini, B. Malaman and B. Roques, *J. Less-Common Met.*, 1990, **160**, 197.
6 C. Geibel, C. Kämmerer, B. Seidel, C. D. Bredl, A. Grauel and F. Steglich, *J. Magn. Magn. Mater.*, 1992, **108**, 207.
7 V. K. Pecharsky, K. A. Gschneidner Jr. and L. L. Miller, *Phys. Rev. B: Condens. Matter*, 1991, **43**, 10906.
8 J.Rodriguez-Carvajal, *Powder diffraction, Satellite Meeting of the 15th Congress of IUCr*, Toulouse, France, 1990, p. 127.
9 P. Schobinger-Papamantellos, J. Rodriguez-Carvajal and K. H. J. Buschow, *J. Alloys Compd.*, 1996, **240**, 85.
10 R. V. Skolozdra, *Stannides of Rare Earth and Transition Metals, Monograph*, Svit, Lviv, Ukraine, 1993, pp. 1–200.
11 J. P. Kuang, H. J. Cui, J. Y. Li, F. M. Yang, H. Nakotte, E. Brück and F. R. de Boer, *J. Magn. Magn. Mater.*, 1992, **104–107**, 1475.
12 T. Takabatake, F. Teshima, H. Fujii, S. Nishigori, T. Suzuki, T. Fujita, Y. Yamaguchi, J. Sakurai and D. Jaccard, *Phys. Rev. B: Condens. Matter*, 1990, **41**, 9607.
13 F. Steglich, P. Hellmann, S. Thomas, P. Gegenwart, A. Link, R. Helfrich, G. Sparn, M. Lang, C. Geibel and W. Assmus, *Physica B*, 1997, **237–238**, 192.
14 T. Takabatake, F. Teshima, H. Fujii, S. Nishigori, T. Suzuki, T. Fujita, Y. Yamaguchi and J. Sakurai, *J. Magn. Magn. Mater.*, 1990, **90–91**, 474.
15 J. Pierre, B. Lambert-Andron, R. V. Skolozdra, J. Rodriguez-Carvajal and K. Kaczmarska, *Physica B*, 1994, **202**, 143.
16 S. Doniach, *Physica B*, 1977, **91**, 231.
17 F. Fourgeot, Thesis, Univ. Bordeaux I, 1996, no. 1576.
18 F. Pourarian and W. E. Wallace, *J. Less-Common Met.*, 1982, **87**, 275.
19 D. Gignoux and J. C. Gomez-Sal, *J. Appl. Phys.*, 1985, **57**, 3125.
20 R. V. Skolozdra, V. M. Mandzyk and L. G. Akelrud, *Kristallografiya*, 1981, **26**, 480.
21 B. Chevalier, J. Garcia Soldevilla, J. I. Espeso, J. Rodriguez Fernandez, J. C. Gomez-Sal and J. Etourneau, *Physica B*, 1999, **259–264**, 44.
22 S. C. Abrahams, J. L. Bernstein, R. C. Sherwood, J. H. Wernick and H. J. Williams, *J. Phys. Chem. Solids*, 1964, **25**, 1069.
23 F. Fourgeot, B. Chevalier, P. Gravereau, L. Fournès and J. Etourneau, *J. Alloys Compd.*, 1995, **218**, 90.
24 I. Higashi, K. Kobayashi, T. Takabatake and M. Kasaya, *J. Alloys Compd.*, 1993, **193**, 300.
25 F. Fourgeot, B. Chevalier, P. Gravereau and J. Etourneau, *Physica B*, 1997, **230–232**, 256.
26 S. K. Dhar, Y. Kimura, M. Kozaki, R. Settai, Y. Önuki, W. Zhao and J. Tang, *J. Phys. Soc. Jpn.*, 1997, **66**, 235.
27 W. P. Beyermann, M. F. Hundley, P. C. Canfield, C. Godart, M. Selsane, Z. Fisk, J. L. Smith and J. D. Thompson, *Physica B*, 1991, **171**, 373.
28 P. Schobinger-Papamantellos, J. Rodriguez-Carvajal, K. Prokes and K. H. J. Buschow, *J. Phys: Condens. Matter*, 1996, **8**, 8635.
29 S. F. Matar, V. Eyert, A. Mavromaras, S. Najm, B. Chevalier and J. Etourneau, *J. Magn. Magn. Mater.*, 1997, **174**, 219.

Paper 9/01903K